Minerals Engineering 156 (2020) 106474

Contents lists available at ScienceDirect

Minerals Engineering

journal homepage: www.elsevier.com/locate/mineng

Selective flotation of apatite from micaceous minerals using patauá palm tree oil collector

Juliana Angélica Evangelista de Carvalho*, Paulo Roberto Gomes Brandão, Andreia Bicalho Henriques, Priscila Silva de Oliveira, Raul Zanoni Lopes Cançado, Gilberto Rodrigues da Silva

Department of Mining Enginneering, Federal University of Minas Gerais, Brazil

ARTICLE INFO

Keywords:
Collector synthesis
Patauá oil
Apatite
Micaceous minerals
Flotation

ABSTRACT

Micaceous minerals are commonly found in phosphate ores, representing a challenge to selectively recover apatite. Aiming at identifying new flotation reagents for the separation of apatite from micaceous minerals, this study investigates the floatability of apatite, biotite and phlogopite in the presence of patauá oil-based collector. The chemical and mineralogical composition, electrokinetic properties and floatability of apatite, biotite and phlogopite in the presence of patauá fatty acid salts, as well as the reagent synthesis and adsorption mechanism were investigated in this work. The collector was successfully synthesized and showed a 90% selectivity gap between apatite and micaceous minerals in microflotation tests, at neutral and alkaline pH. The formation of calcium dicarboxylate was indicated to be the collector adsorption mechanism for apatite, whereas a less significant interaction with interlayer cations exposed during comminution was pointed as the adsorption mechanism for biotite and phlogopite.

1. Introduction

Phosphate ores are an important, non-renewable and currently irreplaceable source of phosphorous for application in the agriculture sector (Bada et al., 2013; Fang and Jun 2011; Horta et al., 2016; Yang et al., 2017), as phosphorus is one of the fertilizers' most important macronutrients for plants, necessary for increasing their productivity and, therefore, ensuring a stable global food supply (Cao et al., 2015; Chen and Graedel, 2015). In fact, currently 80% of the phosphate ores mined worldwide is used to produce phosphoric acid, which is an input in the production of fertilizers (Al-Thyabat et al., 2012; Mohammadkhani et al., 2011).

Apatite is the main valuable phosphorus-bearing mineral in phosphate ores, whereas the non-valuable minerals are mostly carbonates (*e.g.*: calcite and dolomite) and silicates (e.g.: quartz, chert, clays, feldspar and mica) (Liu et al., 2017; Mohammadkhani et al., 2011; Sis and Chander, 2003).

The phosphate ores are usually classed as low (12–16% P_2O_5), medium (17–25% P_2O_5) or high grade (26–35% de P_2O_5) reserves (Mohammadkhani et al., 2011). The main Brazilian phosphate deposits are located in the Alto Paranaíba Igneous Province, in the States of Goiás (Catalão) and Minas Gerais (Araxá and Tapira), and present low grade, which vary from 5 to 15% P_2O_5 (Albuquerque et al., 2012; Zhang et al., 2006). Carbonates and quartz are typically the gangue minerals in these deposits (Hanumantha Rao et al., 1989; Peng and Gu, 2005), although micas also appear in significant amounts in these mineral assemblages, being one of most abundant non-carbonate minerals in carbonatites (Giebel et al., 2019). Phlogopite is one of the main gangue minerals in Goias phoscorites (Albuquerque et al., 2012; Cordeiro et al., 2010; Zhang et al., 2006), whereas biotite and muscovite are present in Minas Gerais deposits (Brod et al., 2001; Seer and Moraes, 2013). Phlogopite and biotite were also identified in Brazilian deposits of minor importance, as Itataia (Albuquerque et al., 2012) and Morro da Mina (Leal Filho et al., 1993).

Micas are a group of minerals which present perfect cleavage in one direction, forming sheets. In this group, the minerals also have a crystalline structure consisting of 2:1 layers (tetrahedral: octahedral) which present a negative structural charge due to the substitutions of Si^{4+} ions by Al^{3+} in the tetrahedral layers or Al^{3+} by Mg^{2+} or Fe^{2+} in the octahedral layers (Parks, 1975; Reynolds, 1980). The charge compensation occurs *via* electrostatic bonds with the cations in between the aluminosilicates layers (Loh and Jarvis, 2010; Parks, 1975).

As a minimum P_2O_5 grade of 30% is required for producing phosphoric acid, phosphate ores usually required concentration, which is

* Corresponding author.
E-mail address: juliana@demin.ufmg.br (J. Angélica Evangelista de Carvalho).

https://doi.org/10.1016/j.mineng.2020.106474
Received 22 December 2019; Received in revised form 21 April 2020; Accepted 19 May 2020
0892-6875/

achieved using flotation (Abouzeid, 2008; Azizi and Larachi, 2018; Cao et al., 2015). In phosphate flotation systems, vegetable oil based fatty acids and their salts are the most common collectors (Brandão et al., 1994; Filippov et al., 2019; Sis and Chander, 2003). These collectors are used to recover apatite in alkaline pH and depressors are used to reduce the flotation of non-valuable minerals (Filippova et al., 2018; Zhang et al., 2006). In these conditions, fatty acids are ionized and the carboxyl group reacts with calcium ions, at the apatite surface and in solution, producing the non-soluble calcium carboxylate (Filippova et al., 2018; Jong et al., 2017). Worldwide, tall oil (a by-product of the paper industry) is the main source of the fatty acids used in flotation plants (El-Shall et al., 2004; Guimarães et al., 2005; Sis and Chander, 2003), although the substitution by alternative vegetable oil sources, *e.g.*: rice, soy bean and grape, is a growing trend currently observed, particularly in Brazil (Cao et al., 2015; Guimarães et al., 2005). In fact, the investigation on alternative vegetable oil sources has been encouraged by tall oil price increases due to paper recycling (Sis and Chander, 2003). Sources recently investigated are: linseed (Linum usitatissimum) (Brandão et al., 1994), babaçu (Orbignya phalerata) (Oliveira et al., 2005), buriti (Mauritia flexuosa), inajá (Attalea maripa), açaí (Euterpe oleracea), passion fruit (Passiflora edulis), andiroba (Carapa guianenses), Brazil nut (Bertholletia excelsa) (Costa et al., 2011), jojoba (Simmondsia chinensis) (Al-Thyabat et al., 2012), coconut (Cocos nucifera) (Albuquerque et al., 2012), macaúba (Acromia aculeata) (Silva et al., 2015a), pequi (Caryocar brasiliense) (Silva et al., 2015b), and patauá (Oenocarpus bataua) (De Oliveira et al., 2019).

Patauá palm trees are found in the Amazon forest in Brazil, French Guiana and Peru. Typically, the fatty acid profile obtained from patauá palm tree oil is similar to that of tall oil as it presents large amounts of unsaturated fatty acids, mainly oleic acid (> 40%) (Balick and Gershoff, 1981; Guimarães et al., 2005; Montúfar et al., 2010). This profile is desired as unsaturated fatty acids are reported to exhibit greater collecting power over apatite (Brandão et al., 1994; Guimarães et al., 2005). The presence of unsaturation in the fatty acid structure not only results in greater solubility (Brandão and Poling, 1982), but it also promotes a partial polymerization between the molecules adsorbed onto the mineral surface, resulting in a mixed film of high stability and hydrophobicity (Brandão, 1988). In the Brazilian phosphate beneficiation plants, the replacement of tall oil by other vegetable oils with similar fatty acid profile is already a consolidated practice (Guimarães et al., 2005). Patauá oil collector has also been reported as a potential collector for phosphate ore flotation, being selective to separate apatite from quartz and calcite at neutral and alkaline pH conditions. Fundamental tests demonstrated that, using low collector concentrations, adsorption took place preferably onto apatite surface. The performance rendered by Patauá oil collector also showed to be greater than that of sodium oleate, as lower dosages of the former reagent was required to achieve selectivity, which indicates lower reagent consumption (De Oliveira et al., 2019). In the Brazilian phosphate beneficiation plants, the replacement of tall oil by other vegetable oils with similar fatty acid profile is already a consolidated practice (Guimarães et al., 2005).

Despite the studies conducted on the selective flotation of mica, such as muscovite and biotite from other silicate minerals in mica schist bed rocks (Hanumantha Rao et al., 1995, 1990), biotite and muscovite from Ca-bearing minerals (Filippov et al., 2012), and the significant number of studies on vegetable oil-based collectors for the flotation of apatite from calcite, dolomite, quartz and other non-valuable minerals (Al-Thyabat et al., 2012; Albuquerque et al., 2012; Brandão et al., 1994; Costa et al., 2011; De Oliveira et al., 2019; Oliveira et al., 2005; Silva et al., 2015a, 2015b), research on the use of fatty acids to separate apatite from micaceous minerals are scarce. In fact, most of siliceous minerals flotation studies are based on cationic collectors as the electrostatic mechanism is well understood to be efficient for this mineral class (Filippov et al., 2012; Hanumantha Rao et al., 1995, 1990; Peng and Gu, 2005). In this sense, based on previous study (De Oliveira et al., 2019), this work expands the study on the use of patauá palm tree oil as a phosphate collector, investigating the selective separation of apatite from the non-valuable biotite and phlogopite, commonly found in Brazilian phosphate deposits.

2. Methodology

2.1. Materials

The apatite, biotite and phlogopite samples were purchased from Luiz Menezes Comércio e Exportação de Minerais Ltda (Belo Horizonte, Brazil). They had their size initially reduced using a hammer, were handpicked to separate impurities, and then pulverized using an agate mortar and pestle to obtain particles in the 212–45 μm size range for microflotation tests and smaller than 38 μm for zeta potential and infrared spectroscopy measurements. The 212–45 μm particle size range was used in the microflotation tests to mimic the coarse friable circuit the Tapira Mineral Complex (CMT), which is one of the most important phosphate ore deposits in Brazil.

The extra virgin patauá oil sample (PO) was supplied by the Amazon Oil Industry Company (Levilândia, Brazil). The collector was produced by saponification of PO at 75 °C using a 2% (w/v) sodium hydroxide / anhydrous ethanol solution under reflux for one hour. At the end of the process, the saponified oil was cooled and filtered, generating a solid (patauá fatty acid salt collector - POC) and a residual liquid fraction (mostly ethanol and glycerol). The solid fraction was dried at 50 °C for 24 h and stored as powder.

2.2. Methods

2.2.1. Characterization

The purity of the mineral samples was evaluated using X-ray powder diffraction (XRD). The tests were conducted in a PW1710 diffractometer (Philips-PANalytical, U.K.) equipped with graphite monochromator crystal and copper X-ray source ($\lambda\ \kappa\alpha\ =\ 1.54$ Å) and performed at 50 kV and 35 mA, with 2θ ranging from 3 to 90°, step size of 0.06° (2 θ) and scan time of 3 s. The chemical analyses were performed using Wavelength Dispersive X-ray Fluorescence (WDXRF) in a PW 2404 spectrometer (Philips-PANalytical, U.K.) equipped with rhodium anode tube. The fusion bead method was used to prepare 2 g samples with $Li_2B_4O_7$.

The electrokinetic properties of the minerals (Zeta Potential) were investigated by electrophoresis using a ZM3-D-G Particle Analyzer (Zeta Meter, U.S.A). The suspensions were prepared by adding 10 mg of < 38 μm mineral sample into 100 mL of pH adjusted 1×10^{-3} M KNO_3 solution (supporting electrolyte). Each suspension was then settled for a period determined by Stokes law in order to obtain particles finer than 2 μm in the final suspension collected for the tests. The pH of suspensions and solutions was adjusted using HNO_3 and KOH.

The fatty acids profile of the patauá palm tree oil (PO) was obtained using Gas Chromatography (GC) of fatty acid methyl esters, with FAME C14-C22 (Supelco cat n∘18917) as standard for the peak identification. These analyses were conducted using a HP7820A Gas Chromatographer (Agilent, U.S.A.) equipped with flame ionizing detector, SGE column, and hydrogen as carrier gas. Iodine and saponification values (IV and SV) were obtained according to the ASTM D5554-15 (Wijs Method) and D5558-95, respectively. These values were also obtained indirectly, based on the fatty acids profile. Acidity index (AI) analyses were performed in compliance with ASTM procedures D5555-95.

The patauá fatty acid salt collector (POC) was characterized by Fourier transform infrared spectroscopy (FTIR) to ensure the efficiency of the saponification reaction. Spectra of both the vegetable oil and the collector were obtained for comparison.

2.2.2. Microflotation

The floatability of apatite, biotite and phlogopite, after conditioning with POC, was investigated in a modified Hallimond tube (Da Silva

et al., 2018). Each test was conducted using 0.5 g single-mineral samples, which were conditioned in the bottom part of the tube with a 40 mL pH adjusted POC concentrated solution for 4 min. Frother was not used in the experiments to avoid synergistic interactions with POC, and also considering the frothing properties expected for fatty acid collectors (Atrafi et al., 2012). The extensor and the top part of the tube were attached, and the suspensions were then completed with pH adjusted reverse osmosis purified water up to a total 310 mL volume. The particles were kept in suspension by agitation using a magnetic stir bar. Nitrogen (N_2) gas was purged through the tube at a flow rate of 40 cm^3/min and flotation was conducted for 1 min. The floated and non-floated products were then filtered, dried and weighed. Floatability was calculated as the weigh percentage floated.

2.2.3. Fourier transform infrared spectroscopy (FTIR)

The collector adsorption onto the surface of apatite, biotite and phlogopite were studied by Fourier transform infrared spectroscopy (FTIR) using an ALPHA II spectrometer (Bruker, U.S.A) in attenuated total reflectance (ATR) mode, with 64 scans within the 4000–675 cm^{-1} range, at 4 cm^{-1} resolution. Measurements were conducted for pure samples and samples conditioned with POC. The mineral samples (10 mg) were conditioned for 30 min in 50 mL of 30 $mg.L^{-1}$ POC solutions, previously pH adjusted. Washing and filtering in 0.05 μm MF-Millipore™ filters were conducted and the solids dried and put in a desiccator for 12 h before the FTIR experiment.

3. Results and discussion

3.1. Characterization

The XRD results were evaluated using the PANalytical X'Pert HighScore and the peaks compared with standards from the ICDD (International Centre for Diffraction Data) PDF-2 database released in 2010. These results, shown in Fig. 1, confirmed the mineral samples presented high purity, which was also confirmed by the WDXRF analyses (Table 1). It can be noted that the apatite sample presented high CaO and P_2O_5 content and the micas had high quantities of Al_2O_3 and SiO_2, for their octahedral and tetrahedral layers, respectively. Biotite and phlogopite samples also presented high Fe_2O_3 and MgO content as a result of the substitution of aluminum ions inside the octahedral sheets, accordingly to the biotite-phlogopite series (Klein and Dutrow, 2012; McKeown et al., 1999). The unexpected CaO content in phlogopite sample are likely to be due to calcium ions located at interlayer positions, in substitution to potassium ions, similarly to what can occur in biotite (Klein and Dutrow, 2012; Reynolds, 1980).

The zeta potential of apatite, biotite and phlogopite were found to be negative in most of the pH conditions investigated, as shown in Fig. 2. The isoelectric point (IEP) of phlogopite and biotite were determined to be at approximately pH 2.1 and 3.0, respectively, which is consistent with previous studies (Bray et al., 2014; Filippov et al., 2012; Rath and Subramanian, 1997; Stenstrom, 1989; Wang and Heiskanen, 1992). The IEP of apatite was observed at approximately pH 2, which is within the wide pH range described for different apatite samples (Filippov et al., 2012; Hu and Xu, 2003; Merma et al., 2013; Owens et al., 2019). The role of supporting electrolyte in zeta potential measurements is to provide enough ions and counter ions for the diffuse double layer, and should not interfere in the values of IEP obtained. If a supporting electrolyte has such effect, it should be considered as a potential determining ion (Fuerstenau and Pradip, 2005) and substituted. The slight differences observed are more likely to be a result of natural variations of chemical composition from one mineral sample to another (Filippova et al., 2014) than as a result of different supporting electrolytes. Table 2 compares the IEP values observed in this work and values found in the Literature.

The patauá oil fatty acid profile, shown in Table 3, presents a predominance of oleic acid and is characteristic of this vegetable oil variety according to AOC standards (Firestone, 2013). The iodine and saponification indexes (Table 4) are also in agreement with specifications of this oil, a result of the fatty acid composition. The small variations are typical of materials of biological origin and are a consequence of natural factors, e.g.: locality, temperature, humidity among others during fruit development.

The acidity index is a parameter which indicates the amount of free fatty acids in the oil sample. A high index is favorable for synthesizing collector reagents as the presence of free fatty acids in the saponification system favor the formation of primary fatty acid salts which act as catalysts (Poulenat et al., 2003; Woollatt, 1985). The greater acidity index observed in the Table 4 is then beneficial.

The ATR-FTIR spectra of PO and POC are shown in Fig. 3, emphasizing the bands related to the carboxyl group. After saponification, it can be noted the disappearance of the 1744 e 1711 cm^{-1} bands (curve a), typical of triglycerides and free fatty acids, respectively, and the appearance of the 1558 cm^{-1} band (curve b), characteristic of sodium fatty acid salts (Mirghani et al., 2002; Schulz and Baranska, 2007). These changes indicate that the saponification occurred completely or almost completely. The additional bands identified in the spectra are related to the hydrocarbon chains from the fatty acid in the oil and in the salt.

3.2. Microflotation

The flotation recovery obtained for phlogopite, biotite and apatite in the microflotation tests as a function of collector concentration and pH are presented in Figs. 4 and 5, respectively. Great selectivity was observed with low POC concentration (2 $mg.L^{-1}$) and could even be enhanced at higher concentrations with no detrimental effects on the

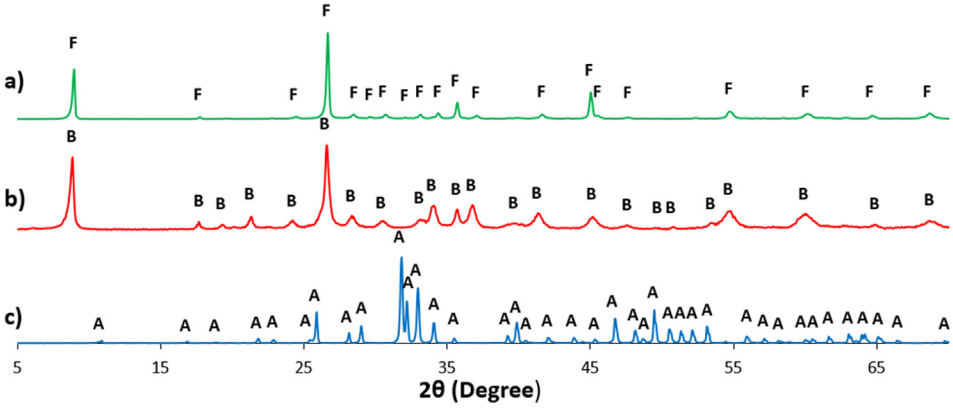

Fig. 1. X-ray diffractogram of a) phlogopite, b) biotite and c) apatite. A: apatite, B: biotite and F: phlogopite (Cu λ κα = 1.54 Å).

Table 1
Chemical composition of the < 212 μm apatite, biotite and phlogopite samples.

Composition (%)	Al_2O_3	CaO	Cr_2O_3	Fe_2O_3	K_2O	MgO	MnO	Na_2O	P_2O_5	SiO_2	TiO_2	ZrO_2	F
Apatite	0.32	53.97	< 0.01	0.19	< 0.01	0.16	0.05	< 0.10	39.92	1.16	< 0.01	–	2.83
Biotite	11.75	0.13	< 0.01	43.59	7.76	0.49	0.35	< 0.10	0.03	30.20	3.41	0.01	–
Phlogopite	13.60	2.14	< 0.01	6.65	10.10	21.74	0.08	0.39	0.59	36.40	2.48	0.03	–

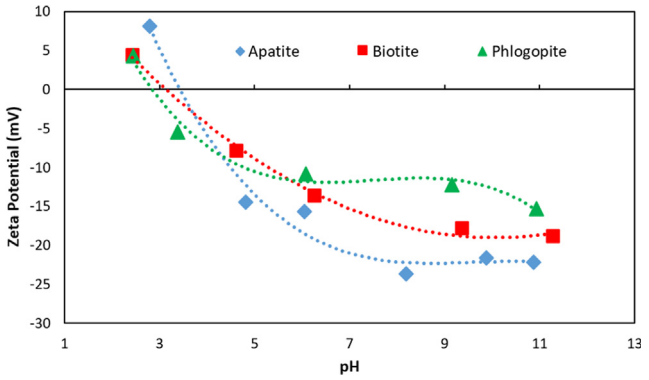

Fig. 2. Zeta potential of apatite, biotite and phlogopite in 1×10^{-3} M KNO_3.

Table 2
IEP values for apatite, biotite e phlogopite.

Mineral	Current Work IEP	Previous Work IEP Reference
Apatite	2	3 (Hu and Xu, 2003) 1–2 (Filippov et al., 2012) < 2.5 (Merma et al., 2013) 2 (Filippova et al., 2014) 1–8.7 (Owens et al., 2019)
Biotite	3	< 4 (Stenstrom,1989) 2.6 (Rath and Subramanian, 1997) < 2 (Filippov et al., 2012) 3 (Bray et al., 2014)
Phlogopite	2.1	2.1 (Wang and Heiskanen, 1992)

floatability of the micaceous minerals. While maximum apatite recovery was found to be approximately 98%, phlogopite and biotite presented approximately 15 and 13% recovery at maximum, respectively. The pH had a small effect on the selectivity window between apatite and the mica minerals, which was maximum at pH 9 and decrease in neutral and more alkaline pH, especially at pH 11 as biotite presented a 28% recovery.

As all the minerals presented negative zeta potential curves in the pH range investigated, in which POC is expected to be dissociated and negatively charged, the collector adsorption onto the surface of the minerals is likely to be of chemical nature. The formation of insoluble calcium carboxylate at the mineral-solution interface has been indicated as the adsorption mechanism in the flotation of minerals containing calcium, such as apatite (Vučinić et al., 2010). As the collector pKa is approximately 4 (Joseph-Soly et al., 2015), the insoluble acid moiety, either as insoluble oil or as colloidal precipitates, is the dominant surfactant species at the system under acidic conditions, which is known to be not as efficient at minerals recovery as carboxylate anions (Joseph-Soly et al., 2015; Quast, 2016).

An increase in pH makes more ionized species available for interacting with calcium ions at the mineral surface and in solution, forming larger amounts of calcium carboxylates (and dicarboxylates) and increasing the apatite recovery. At approximately pH 9, the presence of ionomolecular species and the co-adsorption of neutral acid with oleate ions species help diminishing the repulsion between the collector polar groups and strengthen the hydrophobicity of the mineral surface (Ackerman et al., 1987; Jung et al., 1987; Vučinić et al., 2010).

At higher pH values, the formation of dimeric species can result in an increased adsorption density although it can also lead to a reduced hydrophobicity of the mineral as polar groups may be oriented towards the solution (Cao et al., 2015; Vučinić et al., 2010). Under this condition, it is also likely that the competition between hydroxyl groups and oleate ions at the mineral surface increases, resulting in carboxylate ions as micelles in solution rather than metal carboxylates, which can decrease mineral recovery (Da Silva and Waters, 2018; Joseph-Soly et al., 2015; Quast, 2016, 2012).

The low recovery presented by the micaceous minerals may be due to the low adsorption of POC at the Ca^{2+} and/or Mg^{2+} sites for which the reagent is said to have affinity. In the structure of phlogopite and biotite, the Mg atoms occur in the octahedral layers (McKeown et al., 1999), inside the unity cell, what would make them not available for interaction with the collector. The Ca^{2+} ions among other elements, however, probably occur as an interlayer cation, coordinated to the tetrahedral layers and substituting K^+ (Klein and Dutrow, 2012). The Ca^{2+} position in the cleavage surfaces may favor the adsorption of POC, which might have resulted in the recovery observed for phlogopite.

3.3. Attenuated total reflectance Fourier transform infrared (ATR-FTIR)

The ATR-FTIR spectra of apatite, biotite and phlogopite are shown in Figs. 6, 7 and 8, with emphasis to the 2000–400 cm^{-1} wavelength range. The pure minerals typical bands are presented in curves 6a, 7a e 8a (Balan et al., 2011; Bassett, 1960; Berzina-Cimdina and Borodajenko, 2012; Farmer et al., 1974; Fleet, 2009; van der Marel and Beutelspacher, 1976; Zendah et al., 2012). In the 3100–2800 cm-1 region, typical peaks of hydrocarbon chain groups were observed at nearly 2922 and 2853 cm^{-1} (CH_2) and 2963 cm^{-1}(CH_3) (De Oliveira et al., 2019; Kou et al., 2010; Lerma-García et al., 2010), indicating POC adsorption at the surface of all minerals, with greater intensities in the case of apatite in comparison with biotite and phlogopite. This is consistent with the microflotation results.

The doublet at 1572 and 1536 cm^{-1} is characteristic of calcium dicarboxylate, which adsorbs in multilayers or as precipitated salts (Kou et al., 2010; Lu and Miller, 2002; Mielczarski et al., 1993), and is the predominant species at the hydrophobic apatite surface (Fig. 7).

A calcium dicarboxylate doublet can be observed in the phlogopite FTIR spectra (Fig. 8), indicating the adsorption of POC at interlayer Ca^{2+} sites exposed during fracturing, which is possible since the chemical analyses showed approximately 2% Ca in the phlogopite sample. As similar recoveries were obtained for biotite and carboxylates are not

Table 3
Patauá oil fatty acids profile (%).

Fatty Acid	C12:0	C14:0	C16:0	C16:1	C18:0	C18:1	C18:2	C18:3	C20:0	Other
Oil Sample	0.7	0.5	12.4	0.9	4.5	73.0	7.1	0.4	0.3	–
AOCS(Firestone, 2013)	–	–	9.0	–	6.0	81.0	4.0	–	–	–

Table 4
Chemical parameters of patauá oil.

Chemical parameter	Direct method	Indirect method	Amazon Oil	AOCS (Firestone, 2013)
Iodine Index (g $I_2.g^{-1}$)	78.4 ± 2.7	77.0	75–78	75–80
Saponification Index (mg KOH.g^{-1})	200.3 ± 2.8	193.3	192 – 209	190 – 196
Acidity Index (mg KOH.g^{-1})	28.3 ± 0.4	–	< 20,0	–

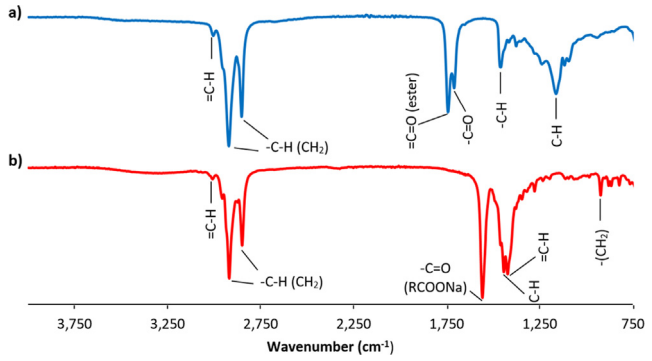

Fig. 3. ATR-FTIR spectra of a) patauá oil (PO) and b) patauá collector (POC).

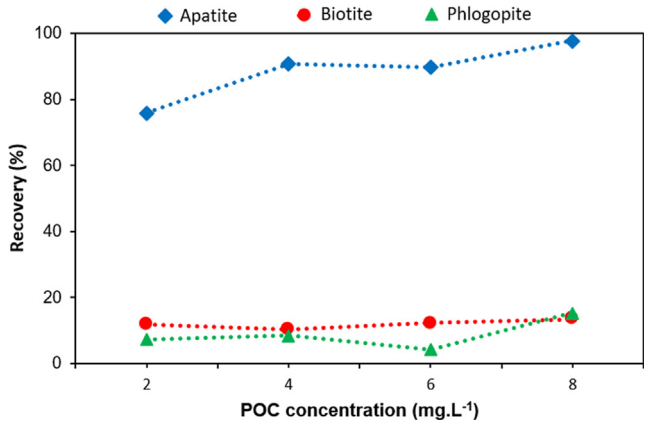

Fig. 4. Mineral recovery as a function of POC concentration at pH 9.

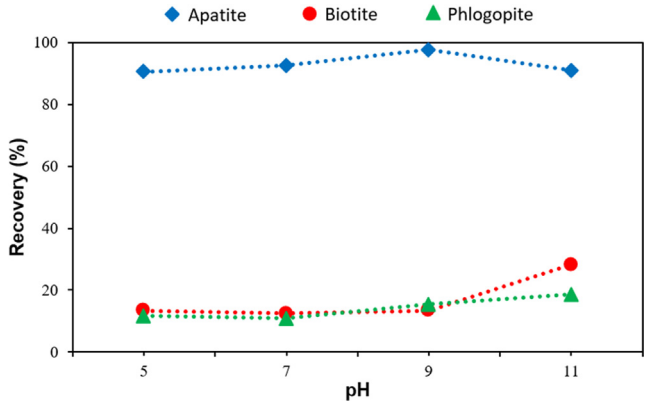

Fig. 5. Mineral recovery as a function of pH for systems with 8 mg.L^{-1} POC.

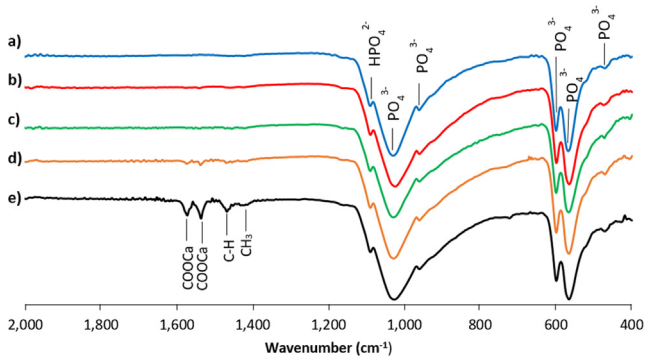

Fig. 6. ATR-FTIR spectra of apatite: a) pure, and conditioned with POC at pH b) 5, c) 7, d) 9 and e) 11.

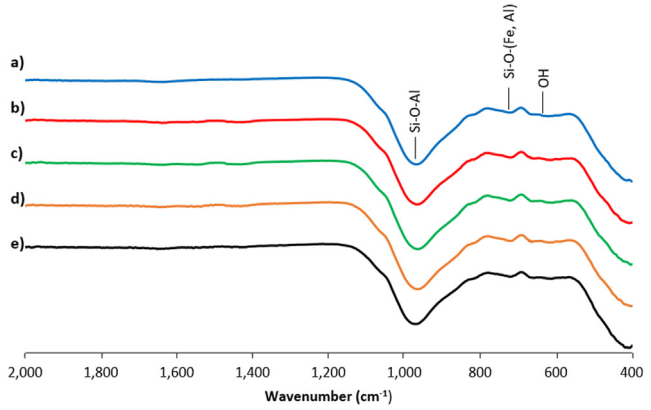

Fig. 7. ATR-FTIR spectra of biotite: a) pure, and conditioned with POC at pH b) 5, c) 7, d) 9 and e) 11.

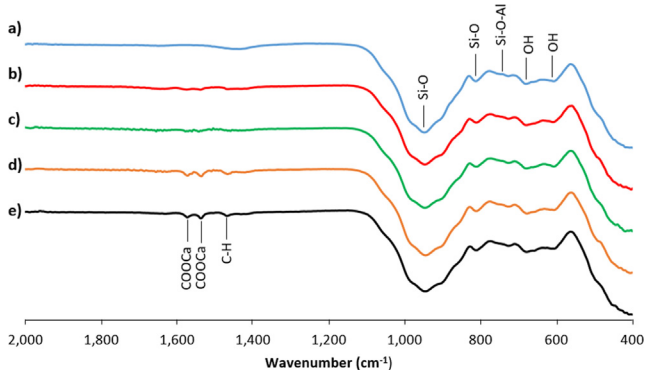

Fig. 8. ATR-FTIR spectra of phlogopite: a) pure, and conditioned with POC at pH b) 5, c) 7, d) 9 and e) 11.

noted in its FTIR spectra (Fig. 7), potassium ion substitutions might also have taken place at interlayer sites leading to interactions of POC with different cations, such as barium, which is commonly observed for biotite (Deng et al., 2019; Klein and Dutrow, 2012).

In the apatite and phlogopite spectra, an increase in the intensity of carboxylate peaks was also observed with an increase in pH. As discussed before, the more alkaline the medium, the more POC ionized species are available to adsorb onto the mineral surfaces. The ionized species, nevertheless, consist of monomeric and dimeric species, and soap-acid complex (Vučinić et al., 2010), which are not possible to differentiate using FTIR analyses, as they anchor similarly onto the minerals surfaces and generate the same peaks. In the biotite spectra, the absence of peaks in the carboxylate region may be a result of a low

adsorption density, as the microflotation results indicate POC adsorption should not be completely absent.

4. Conclusions

This study showed that a selective fatty acid salt collector for apatite flotation can be synthesized from patauá palm tree oil, an abundant vegetable oil source found in the Amazon region. The collector has great potential for application in the flotation of phosphate ores with significant micaceous mica content, whereas the use of patauá oil in the reagents industry can generate economic growth in the Amazon region. Bench flotation tests should be conducted with ore samples to further investigate the collector performance.

CRediT authorship contribution statement

Juliana Angélica Evangelista de Carvalho: Conceptualization, Methodology. **Paulo Roberto Gomes Brandão:** Investigation. **Andreia Bicalho Henriques:** Supervision. **Priscila Silva de Oliveira:** Writing, Data analysis. **Raul Zanoni Lopes Cançado:** Validation. **Gilberto Rodrigues da Silva:** Reviewing, Editing.

Declaration of Competing Interest

The authors declare that they have no known competing financial interests or personal relationships that could have appeared to influence the work reported in this paper.

Acknowledgements

The authors thank all who collaborated in this work and acknowledge the financial support from UFMG, Engineering School, PPGEM and CAPES / PROEX.

References

Abouzeid, A.Z.M., 2008. Physical and thermal treatment of phosphate ores - An overview. Int. J. Miner. Process. 85, 59–84. https://doi.org/10.1016/j.minpro.2007.09.001.

Ackerman, P.K., Harris, G.H., Klimpel, R.R., Aplan, F.F., 1987. Evaluation of Flotation Collectors for Copper Sulfides and Pyrite, II. Non-Sulfhydryl Collectors. Int. J. Miner. Process. 21, 129–140.

Al-Thyabat, S., Hararеh, M., Tarawneh, K., Al-Zoubi, H., 2012. Preliminary investigations into the use of jojoba oil as a possible collector in phosphate flotation, in: Zhang, P., Miller, J., El-Shall, H. (Eds.), Beneficiation of Phosphates: New Thought, New Technology, New Development. Society for Mining, Metallurgy, and Exploration, Englewood, pp. 343–352.

Albuquerque, R.O., Peres, A.E.C., Aquino, J.A., Praes, P.E., Pereira, C.A., 2012. Pilot scale direct flotation of a phosphate ore with silicate-carbonate gangue. Procedia Eng. 46, 105–110. https://doi.org/10.1016/j.proeng.2012.09.452.

Atrafi, A., Gomez, C.O., Finch, J.A., Pawlik, M., 2012. Frothing behavior of aqueous solutions of oleic acid. Miner. Eng. 36–38, 138–144. https://doi.org/10.1016/j.mineng.2012.03.020.

Azizi, D., Larachi, F., 2018. Surface interactions and flotation behavior of calcite, dolomite and ankerite with alkyl hydroxamic acid bearing collector and sodium silicate. Colloids Surfaces A Physicochem. Eng. Asp. 537, 126–138. https://doi.org/10.1016/j.colsurfa.2017.09.054.

Bada, S., Gcanga, S., Falcon, L., Falcon, R., Makhula, M., 2013. Electrostatic concentration of phosphate flotation concentrate. Int. J. Min. Sci. Technol. 23, 403–406. https://doi.org/10.1016/j.ijmst.2013.05.013.

Balan, E., Delattre, S., Roche, D., Segalen, L., Morin, G., Guillaumet, M., Blanchard, M., Lazzeri, M., Brouder, C., Salje, E.K.H., 2011. Line-broadening effects in the powder infrared spectrum of apatite. Phys. Chem. Miner. 38, 111–122. https://doi.org/10.1007/s00269-010-0388-x.

Balick, M.J., Gershoff, S.N., 1981. Nutritional evaluation of the Jessenia bataua palm: Source of high quality protein and oil from tropical America. Econ. Bot. 35, 261–271. https://doi.org/10.1007/BF02859117.

Bassett, W.A., 1960. Role of hidroxyl orientation in mica alternation. Bulletin of The Geological Society of America 71, 449–456.

Berzina-Cimdina, L., Borodajenko, N., 2012. Research of Calcium Phosphates Using Fourier Transform Infrared Spectroscopy, in: Theophile, T. (Ed.), Infrared Spectroscopy - Materials Science, Engineering and Technology. InTech, Rijeka, pp. 123–148. https://doi.org/10.5772/36942.

Brandão, P.R.G., 1988. A oxidação do oleato durante a flotação de oxi-minerais e suas conseqüencias. XIII Encontro Nacional de Tratamento de Minérios. 983–998.

Brandão, P.R.G., Caires, L.G., Queiroz, D.S.B., 1994. Vegetable lipid oil-based collectors in the flotation of apatite ores. Miner. Eng. 7, 917–925. https://doi.org/10.1016/0892-6875(94)90133-3.

Brandão, P.R.G., Poling, G.W., 1982. Anionic Flotation of Magnesite. Can. Metall. Q. 21, 211–220. https://doi.org/10.1179/cmq.1982.21.3.211.

Bray, A.W., Benning, L.G., Bonneville, S., Oelkers, E.H., 2014. Biotite surface chemistry as a function of aqueous fluid composition. Geochim. Cosmochim. Acta 128, 58–70. https://doi.org/10.1016/j.gca.2013.12.002.

Brod, J.A., Gaspar, J.C., De Araújo, D.P., Gibson, S.A., Thompson, R.N., Junqueira-Brod, T.C., 2001. Phlogopite and tetra-ferriphlogopite from Brazilian carbonatite complexes: Petrogenetic constraints and implications for mineral-chemistry systematics. J. Asian Earth Sci. 19, 265–296. https://doi.org/10.1016/S1367-9120(00)00047-X.

Cao, Q., Cheng, J., Wen, S., Li, C., Bai, S., Liu, D., 2015. A mixed collector system for phosphate flotation. Miner. Eng. 78, 114–121. https://doi.org/10.1016/j.mineng.2015.04.020.

Chen, M., Graedel, T.E., 2015. The potential for mining trace elements from phosphate rock. J. Clean. Prod. 91, 337–346. https://doi.org/10.1016/j.jclepro.2014.12.042.

Cordeiro, P.F.O., Brod, J.A., Dantas, E.L., Barbosa, E.S.R., 2010. Mineral chemistry, isotope geochemistry and petrogenesis of niobium-rich rocks from the Catalão I carbonatite-phoscorite complex, Central Brazil. Lithos 118, 223–237. https://doi.org/10.1016/j.lithos.2010.04.007.

Costa, D.S., Alves, A.S., Budke, R., Mendes, R.M.M., Peres, A.E.C., 2011. Flotabilidade de apatita usando óleos vegetais da Amazônia como coletores, in: XXIV Encontro Nacional de Tratamento de Minérios e Metalurgia Extrativa. Salvador, pp. 237–244.

Da Silva, G.R., Espiritu, E.R.L., Mohammadi-Jam, S., Waters, K.E., 2018. Surface characterization of microwave-treated chalcopyrite. Colloids Surfaces A 555, 407–417. https://doi.org/10.1016/j.colsurfa.2018.06.078.

Da Silva, G.R., Waters, K.E., 2018. The effects of microwave irradiation on the floatability of chalcopyrite, pentlandite and pyrrhotite. Adv. Powder Technol. 29, 3049–3061. https://doi.org/10.1016/j.apt.2018.07.025.

De Oliveira, P., Mansur, H., Mansur, A., Da Silva, G., Peres, A., 2019. Apatite flotation using pataua palm tree oil as collector. J. Mater. Res. Technol. 8, 4612–4619. https://doi.org/10.1016/j.jmrt.2019.08.005.

Deng, J., Liu, C., Yang, S., Li, H., Liu, Y., 2019. Flotation separation of barite from calcite using acidified water glass as the depressant. Colloids Surfaces A Physicochem. Eng. Asp. 579, 123605. https://doi.org/10.1016/j.colsurfa.2019.123605.

El-Shall, H., Zhang, P., Abdel-Khalek, N., El-Mofty, S., 2004. Beneficiation technology of phosphates: challenges and solutions. Miner. Metall. Process. 21, 17–26.

Fang, G., Jun, L., 2011. Selective separation of silica from a siliceous–calcareous phosphate rock. Min. Sci. Technol. 21, 135–139. https://doi.org/10.1016/j.mstc.2010.12.018.

Farmer, V.C., Russell, J.D., Hadni, A., Lazarev, A.N., White, W.B., Moenke, H.H.W., Griffith, W.P., Ryskin, Y.I., Ross, S.D., Strens, R.G.J., Henning, O., Freund, F., Parke, S., 1974. The infrared spectra of minerals. Mineralogical Society, London.

Filippov, L.O., Duverger, A., Filippova, I.V., Kasaini, H., Thiry, J., 2012. Selective flotation of silicates and Ca-bearing minerals: The role of non-ionic reagent on cationic flotation. Miner. Eng. 36–38, 314–323. https://doi.org/10.1016/j.mineng.2012.07.013.

Filippov, L.O., Filippova, I.V., Lafhaj, Z., Fornasiero, D., 2019. The role of a fatty alcohol in improving calcium minerals flotation with oleate. Colloids Surfaces A 560, 410–417. https://doi.org/10.1016/j.colsurfa.2018.10.022.

Filippova, I.V., Filippov, L.O., Duverger, A., Severov, V.V., 2014. Synergetic effect of a mixture of anionic and nonionic reagents: Ca mineral contrast separation by flotation at neutral pH. Miner. Eng. 66, 135–144. https://doi.org/10.1016/j.mineng.2014.05.009.

Filippova, I.V., Filippov, L.O., Lafhaj, Z., Barres, O., Fornasiero, D., 2018. Effect of calcium minerals reactivity on fatty acids adsorption and flotation. Colloids Surfaces A Physicochem. Eng. Asp. 545, 157–166. https://doi.org/10.1016/j.colsurfa.2018.02.059.

Firestone, D., 2013. Physical and Chemical Characteristics of Oils, Fats, and Waxes, 3rd, Ed. ed. AOCS Press, Urbana, Illinois.

Fleet, M.E., 2009. Infrared spectra of carbonate apatites: ν2-Region bands. Biomaterials 30, 1473–1481. https://doi.org/10.1016/j.biomaterials.2008.12.007.

Fuerstenau, D.W., Pradip, 2005. Zeta potentials in the flotation of oxide and silicate minerals. Adv. Colloid Interface Sci. 114–115, 9–26. https://doi.org/10.1016/j.cis.2004.08.006.

Giebel, R.J., Marks, M.A.W., Gauert, C.D.K., Markl, G., 2019. A model for the formation of carbonatite-phoscorite assemblages based on the compositional variations of mica and apatite from the Palabora Carbonatite Complex, South Africa. Lithos 324–325, 89–104. https://doi.org/10.1016/j.lithos.2018.10.030.

Guimarães, R.C., Araujo, A.C., Peres, A.E.C., 2005. Reagents in igneous phosphate ores flotation. Miner. Eng. 18, 199–204. https://doi.org/10.1016/j.mineng.2004.08.022.

Hanumantha Rao, K., Antti, B.-M., Forssberg, E., 1989. Flotation of phosphatic material containing carbonatic gangue using sodium oleate as collector and sodium silicate as modifier. Int. J. Miner. Process. 26, 123–140. https://doi.org/10.1016/0301-7516(89)90047-1.

Hanumantha Rao, K., Antti, B.-M., Forssberg, K.S.E., 1990. Flotation of mica minerals and selectivity between muscovite and biotite while using mixed anionic/cationic collectors. Miner. Metall. Process. 7, 127–132. https://doi.org/10.1007/BF03403286.

Hanumantha Rao, K., Cases, J.M., Barres, O., Forssberg, K.S.E., 1995. Flotation, electrokinetic and FT-IR studies of mixed anionic/cationic collectors in muscovite-biotite system. In: Mehrotra, S.P., Shekhar, R. (Eds.), Mineral Processing: Recent Advances and Future Trends. Allied Publishers Ltd, New Dehli, pp. 22–44.

Horta, D., Monte, M.B. de M., Leal Filho, L. de S., 2016. The effect of dissolution kinetics on flotation response of apatite with sodium oleate. Int. J. Miner. Process. 146, 97–104. https://doi.org/10.1016/j.minpro.2015.12.003.

Hu, Y., Xu, Z., 2003. Interactions of amphoteric amino phosphoric acids with calcium-containing minerals and selective flotation. Int. J. Miner. Process. 72, 87–94. https://doi.org/10.1016/S0301-7516(03)00089-9.
Jong, K., Han, Y., Ryom, S., 2017. Flotation mechanism of oleic acid amide on apatite. Colloids Surfaces A Physicochem. Eng. Asp. 523, 127–131. https://doi.org/10.1016/j.colsurfa.2016.11.038.
Joseph-Soly, S., Quast, K., Connor, J.N., 2015. Effects of Eh and pH on the oleate flotation of iron oxides. Miner. Eng. 83, 97–104. https://doi.org/10.1016/j.mineng.2015.08.014.
Jung, R.F., James, R.O., Healy, T.W., 1987. Adsorption, precipitation, and electrokinetic processes in the iron oxide (Goethite)-oleic acid-oleate system. J. Colloid Interface Sci. 118, 463–472. https://doi.org/10.1016/0021-9797(87)90482-6.
Klein, C., Dutrow, B., 2012. Manual de Ciência dos Minerais, 23rd ed. Bookman, Porto Alegre.
Kou, J., Tao, D., Xu, G., 2010. Fatty acid collectors for phosphate flotation and their adsorption behavior using QCM-D. Int. J. Miner. Process. 95, 1–9. https://doi.org/10.1016/j.minpro.2010.03.001.
Leal Filho, L.S., Assis, S.M., Araujo, A.C., Chaves, A.P., 1993. Process mineralogy studies for optimizing the flotation performance of two refractory phosphate ores. Miner. Eng. 6, 907–916. https://doi.org/10.1016/0892-6875(93)90063-S.
Lerma-García, M.J., Ramis-Ramos, G., Herrero-Martínez, J.M., Simó-Alfonso, E.F., 2010. Authentication of extra virgin olive oils by Fourier-transform infrared spectroscopy. Food Chem. 118, 78–83. https://doi.org/10.1016/j.foodchem.2009.04.092.
Liu, X., Ruan, Y., Li, C., Cheng, R., 2017. Effect and mechanism of phosphoric acid in the apatite/dolomite flotation system. Int. J. Miner. Process. 167, 95–102. https://doi.org/10.1016/j.minpro.2017.08.006.
Loh, S., Jarvis, S.P., 2010. Visualization of Ion Distribution at the Mica − Electrolyte Interface. Langmuir 26, 9176–9178. https://doi.org/10.1021/la1011378.
Lu, Y., Miller, J.D., 2002. Carboxyl Stretching Vibrations of Spontaneously Adsorbed and LB-Transferred Calcium Carboxylates as Determined by FTIR Internal Reflection Spectroscopy. J. Colloid Interface Sci. 256, 41–52. https://doi.org/10.1006/jcis.2001.8112.
McKeown, D.A., Bell, M.I., Etz, E.S., 1999. Raman spectra and vibrational analysis of the trioctahedral mica phlogopite. Am. Mineral. 84, 970–976. https://doi.org/10.2138/am-1999-5-633.
Merma, A.G., Torem, M.L., Morán, J.J.V., Monte, M.B.M., 2013. On the fundamental aspects of apatite and quartz flotation using a Gram positive strain as a bioreagent. Miner. Eng. 48, 61–67. https://doi.org/10.1016/j.mineng.2012.10.018.
Mielczarski, J.A., Cases, J.M., Bouquet, E., Barres, O., Delon, J.F., 1993. Nature and Structure of Adsorption Layer on Apatite Contacted with Oleate Solution. 1. Adsorption and Fourier Transform Infrared Reflection Studies. Langmuir 9, 2370–2382. https://doi.org/10.1021/la00033a020.
Mirghani, M.E.S., Che Man, Y.B., Jinap, S., Baharin, B.S., Bakar, J., 2002. FTIR spectroscopic determination of soap in refined vegetable oils. JAOCS. J. Am. Oil Chem. Soc. 79, 111–116. https://doi.org/10.1007/s11746-002-0443-4.
Mohammadkhani, M., Noaparast, M., Shafaei, S.Z., Amini, A., Amini, E., Abdollahi, H., 2011. Double reverse flotation of a very low grade sedimentary phosphate rock, rich in carbonate and silicate. Int. J. Miner. Process. 100, 157–165. https://doi.org/10.1016/j.minpro.2011.06.001.
Montúfar, R., Laffargue, A., Pintaud, J.C., Hamon, S., Avallone, S., Dussert, S., 2010. Oenocarpus bataua Mart. (arecaceae): Rediscovering a source of high oleic vegetable oil from Amazonia. JAOCS. J. Am. Oil Chem. Soc. 87, 167–172. https://doi.org/10.1007/s11746-009-1490-4.
Oliveira, J.A., Luz, J.A.M., Ferreira, E.E., 2005. Grau de saponificação de óleos vegetais na flotação de apatita, in: XXI Encontro Nacional de Tratamento de Minérios e Metalurgia Extrativa. Natal, pp. 259–265.
Owens, C.L., Nash, G.R., Hadler, K., Fitzpatrick, R.S., Anderson, C.G., Wall, F., 2019. Apatite enrichment by rare earth elements : A review of the effects of surface properties. Adv. Colloid Interface Sci. 265, 14–28. https://doi.org/10.1016/j.cis.2019.01.004.
Parks, G.A., 1975. Adsorption in The Marine Environment. In: Riley, J.P., Skirrow, G. (Eds.), Chemical Oceanography. Academic Press, London, pp. 241–308.
Peng, F.F., Gu, Z., 2005. Processing Florida dolomitic phosphate pebble in a double reverse fine flotation process. Miner. Metall. Process. 22, 23–30. https://doi.org/10.1007/bf03403192.
Poulenat, G., Sentenac, S., Mouloungui, Z., 2003. Fourier-Transform Infrared Spectra of Fatty Acid Salts - Kinetics of High-Oleic Sunflower Oil Saponification. J. Surfactants Deterg. 6, 305–310. https://doi.org/10.1007/s11743-003-0274-1.
Quast, K., 2016. The use of zeta potential to investigate the pKa of saturated fatty acids. Adv. Powder Technol. 27, 207–214. https://doi.org/10.1016/j.apt.2015.12.003.
Quast, K., 2012. Effect of 25 %Goethite on the Hydrophobicity and Oleate Flotation of Hematite. Int. J. Min. Eng. Miner. Process. 1, 31–37. https://doi.org/10.5923/j.mining.20120102.02.
Rath, R.K., Subramanian, S., 1997. Studies on adsorption of guar gum onto biotite mica. Miner. Eng. 10, 1405–1420. https://doi.org/10.1016/S0892-6875(97)00130-1.
Reynolds, R.C., 1980. Interstratified Clay Minerals. In: Brindley, G.W., Brown, G. (Eds.), Crystal Structures of Clay Minerals and Their X-Ray Identification. Mineralogical Society of Great Britain and Ireland, London, pp. 249–304.
Schulz, H., Baranska, M., 2007. Identification and quantification of valuable plant substances by IR and Raman spectroscopy. Vib. Spectrosc. 43, 13–25. https://doi.org/10.1016/j.vibspec.2006.06.001.
Seer, H.J., de Moraes, L.C., 2013. Within plate, arc, and collisional Neoproterozoic granitic magmatism in the Araxá Group, Southern Brasília belt, Minas Gerais. Brazil. Brazilian J. Geol. 43, 333–354. https://doi.org/10.5327/Z2317-48892013000200010.
Silva, A.C., Silva, E.M.S., Rocha, T.W.P., 2015a. Microflotação de apatita utilizando óleo da castanha de macaúba (Acrocomia Aculeata) como coletor. Tecnol. em Metal. Mater. e Mineração 12, 146–152. https://doi.org/10.4322/2176-1523.0836.
Silva, A.C., Silva, E.M.S., Silva, T.C., Alves, B.E., 2015b. Apatite microflotation using pequi oil. Miner. Process. Extr. Metall. 124, 233–239. https://doi.org/10.1179/1743285515Y.0000000015.
Sis, H., Chander, S., 2003. Reagents used in the flotation of phosphate ores: a critical review. Miner. Eng. 16, 577–585. https://doi.org/10.1016/S0892-6875(03)00131-6.
Stenstrom, T.A., 1989. Bacterial Hydrophobicity, an Overall Parameter for the Measurement of Adhesion Potential to Soil Particles. Appl. Environ. Microbiol. 55, 142–147.
van der Marel, H.W., Beutelspacher, H., 1976. Admixtures. In: van der Marel, H.W., Beutelspacher, H. (Eds.), Atlas of Infrared Spectroscopy of Clay Minerals and Their Admixtures. Elsevier Scientific Publishing Company, Amsterdam, pp. 241–274.
Vučinić, D.R., Radulović, D.S., Deušić, S.Đ., 2010. Electrokinetic properties of hydroxyapatite under flotation conditions. J. Colloid Interface Sci. 343, 239–245. https://doi.org/10.1016/j.jcis.2009.11.024.
Wang, Q., Heiskanen, K., 1992. Dispersion selectivity and heterocoagulation in apatite-hematite-phlogopite fine particle suspensions I. Dispersion of single minerals. Int. J. Miner. Process. 35, 121–131. https://doi.org/10.1016/0301-7516(92)90008-K.
Woollatt, E., 1985. Manufacture of soaps, other detergents and glycerine. E. Horwood, Chichester.
Yang, X., Liu, S., Liu, G., Zhong, H., 2017. A DFT study on the structure–reactivity relationship of aliphatic oxime derivatives as copper chelating agents and malachite flotation collectors. J. Ind. Eng. Chem. 46, 404–415. https://doi.org/10.1016/j.jiec.2016.11.010.
Zendah, H., Khattech, I., Jemal, M., 2012. Synthesis, characterization, and thermochemistry of acid attack of “B” type carbonate fluorapatites. J. Therm. Anal. Calorim. 109, 855–861. https://doi.org/10.1007/s10973-011-1858-1.
Zhang, P., Wiegel, R., El-Shall, H., 2006. Phosphate Rock, in: Kogel, J.E., Trivedi, N.C., Barker, J.M., Krukowski, S.T. (Eds.), Industrial Minerals and Rocks – Commodities, Markets and Uses. Society for Mining, Metallurgy, and Exploration, Littleton, pp. 704–722.